COSMIC BACKGROUND RADIATION

To reduce the size of this section's PostScript file, we have divided it into two PostScript files. We present the following index:

PART 1

Page #	Section name	
1	19.1	Introduction
1	19.2	The CMB frequency spectrum

PART 2

Page #	Section name	
6	19.3	Deviations from isotropy
11		References

19.3. Deviations from isotropy

Penzias and Wilson reported that the CMB was isotropic and unpolarized to the 10% level. Current observations show that the CMB is unpolarized at the 10^{-5} level but has a dipole anisotropy at the 10^{-3} level, with smaller-scale anisotropies at the 10^{-5} level. Standard theories predict anisotropies in linear polarization well below currently achievable levels, but temperature anisotropies of roughly the amplitude now being detected.

It is customary to express the CMB temperature anisotropies on the sky in a spherical harmonic expansion,

$$\frac{\Delta T}{T}(\theta,\phi) = \sum_{\ell m} a_{\ell m} Y_{\ell m}(\theta,\phi) \ , \tag{19.8}$$

and to discuss the various multipole amplitudes. The power at a given angular scale is roughly $\ell \sum_m |a_{\ell m}|^2 / 4\pi$, with $\ell \sim 1/\theta$.

19.3.1. ***The dipole***: The largest anisotropy is in the $\ell = 1$ (dipole) first spherical harmonic, with amplitude at the level of $\Delta T/T = 1.23 \times 10^{-3}$. The dipole is interpreted as the result of the Doppler shift caused by the solar system motion relative to the nearly isotropic blackbody field. The motion of the observer (receiver) with velocity $\beta = v/c$ relative to an isotropic Planckian radiation field of temperature T_0 produces a Doppler-shifted temperature

$$\begin{aligned} T(\theta) &= T_0(1-\beta^2)^{1/2}/(1-\beta\cos\theta) \\ &= T_0 \left(1 + \beta\cos\theta + (\beta^2/2)\cos 2\theta + O(\beta^3)\right) \ . \end{aligned} \tag{19.9}$$

The implied velocity [11,14] for the solar-system barycenter is $\beta = 0.001236 \pm 0.000002$ (68% CL) or $v = 371 \pm 0.5\,\mathrm{km\,s^{-1}}$, assuming a value $T_0 = 2.728 \pm 0.002\,\mathrm{K}$, towards $(\alpha,\delta) = (11.20^\mathrm{h} \pm 0.01^\mathrm{h}, -7.22^\circ \pm 0.08^\circ)$, or $(\ell, b) = (264.31^\circ \pm 0.17^\circ, 48.05^\circ \pm 0.10^\circ)$. Such a solar-system velocity implies a velocity for the Galaxy and the Local Group of galaxies relative to the CMB. The derived velocity is $v_\mathrm{LG} = 627 \pm 22\,\mathrm{km\,s^{-1}}$ toward $(\ell, b) = (276^\circ \pm 3^\circ, 30^\circ \pm 3^\circ)$, where most of the error comes from uncertainty in the velocity of the solar system relative to the Local Group.

The Doppler effect of this velocity and of the velocity of the Earth around the Sun, as well as any velocity of the receiver relative to the Earth, is normally removed for the purposes of CMB anisotropy study. The resulting high degree of CMB isotropy is the strongest evidence for the validity of the Robertson-Walker metric.

19.3.2. ***The quadrupole***: The rms quadrupole anisotropy amplitude is defined through $Q^2_{\rm rms}/T^2_\gamma = \sum_m |a_{2m}|^2 /4\pi$. The current estimate of its value is $4\,\mu{\rm K} \leq Q_{\rm rms} \leq 28\,\mu{\rm K}$ for a 95% confidence interval [15]. The uncertainty here includes both statistical errors and systematic errors, which are dominated by the effects of galactic emission modelling. This level of quadrupole anisotropy allows one to set general limits on anisotropic expansion, shear, and vorticity; all such dimensionless quantities are constrained to be less than about 10^{-5}.

For specific homogeneous cosmologies, fits to the whole anisotropy pattern allow stringent limits to be placed on, for example, the global rotation at the level of about 10^{-7} of the expansion rate [16].

19.3.3. ***Smaller angular scales***: The COBE-discovered [17] higher-order ($\ell > 2$) anisotropy is interpreted as being the result of perturbations in the energy density of the early Universe, manifesting themselves at the epoch of the CMB's last scattering. Hence the detection of these anisotropies has provided evidence for the existence of primordial density perturbations which grew through gravitational instability to form all the structure we observe today.

In the standard scenario the last scattering takes place at a redshift of approximately 1100, at which epoch the large number of photons was no longer able to keep the hydrogen sufficiently ionized. The optical thickness of the cosmic photosphere is roughly $\Delta z \sim 100$ or about 5 arcminutes, so that features smaller than this size are damped.

Anisotropies are observed on angular scales larger than this damping scale (see Fig. 19.5 and 19.6), and are consistent with those expected from an initially scale-invariant power spectrum (flat = independent of scale) of potential and thus metric fluctuations. It is believed that the large scale structure in the Universe developed through the process of gravitational instability, where small primordial perturbations in energy density were amplified by gravity over the course of time. The initial spectrum of density perturbations can evolve significantly in the epoch $z > 1100$ for causally connected regions (angles $\lesssim 1^\circ\ \Omega_{\rm tot}^{1/2}$). The primary mode of evolution is through adiabatic (acoustic) oscillations, leading to a series of peaks that encode information about the perturbations and geometry of the Universe, as well as information on Ω_0, Ω_B, Ω_Λ (cosmological constant), and H_0 [18]. The location of the first acoustic peak is predicted to be at $\ell \sim 220\ \Omega_{\rm tot}^{-1/2}$ or $\theta \sim 0.3^\circ\ \Omega_{\rm tot}^{1/2}$ and its amplitude is a calculable function of the parameters.

Theoretical models generally predict a power spectrum in spherical harmonic amplitudes, since the models lead to primordial fluctuations and thus $a_{\ell m}$ that are Gaussian random fields, and hence the power spectrum in ℓ is sufficient to characterize the results. The power at each ℓ is $(2\ell+1)C_\ell/(4\pi)$, where $C_\ell \equiv \left\langle |a_{\ell m}|^2 \right\rangle$ and a statistically isotropic sky means that all m's are equivalent. For an idealized full-sky observation, the variance of each measured C_ℓ is $[2/(2\ell+1)]C_\ell^2$. This sampling variance (known as cosmic variance) comes about because each C_ℓ is chi-squared distributed with $(2\ell+1)$ degrees of freedom for our observable volume of the Universe [19].

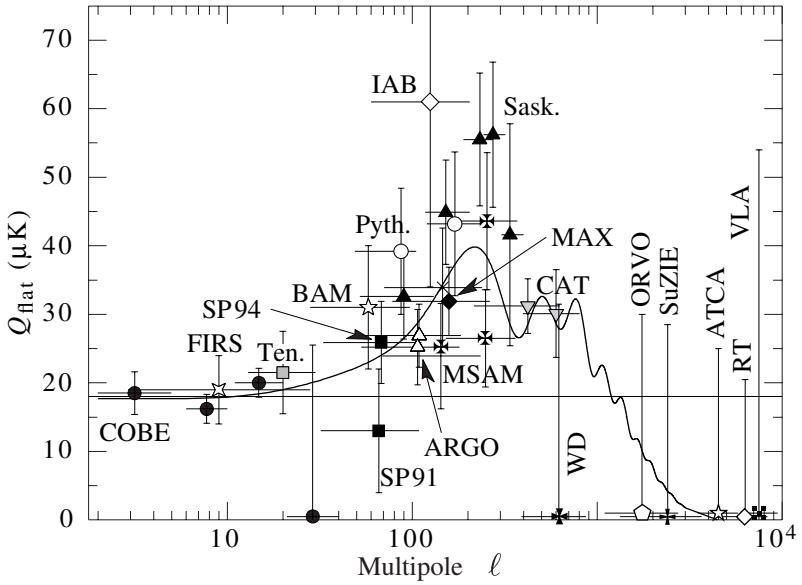

Figure 19.5: Current status of CMB anisotropy observations, adapted from Scott, Silk, & White (1995) [18]. This is a representation of the results from COBE, together with a wide range of ground- and balloon-based experiments which have operated in the last few years. Plotted are the quadrupole amplitudes for a flat (unprocessed scale-invariant spectrum of primordial perturbations, *i.e.*, a horizontal line) anisotropy spectrum that would give the observed results for each experiment. In other words each point is the normalization of a flat spectrum derived from the individual experiments. The vertical error bars represent estimates of 68% CL, while the upper limits are at 95% CL. Horizontal bars indicate the range of ℓ values sampled. The curve indicates the expected spectrum for a standard CDM model ($\Omega_0 = 1, \Omega_B = 0.05, h = 0.5$), although true comparison with models should involve convolution of this curve with each experimental filter function. The dashed line is the best fitted flat spectrum derived from the COBE data alone [24]. (References for this figure are at the end of this section under "CMB Anisotropy References.")

Thomson scattering of the anisotropic radiation field also generates linear polarization at the roughly 5% level [20]. Although difficult to detect, the polarization signal should act as a strong confirmation of the general paradigm.

Figure 19.7 shows the theoretically predicted anisotropy power spectrum for a sample of models, plotted as $\ell(\ell+1)C_\ell$ versus ℓ which is the power per logarithmic interval in ℓ or, equivalently, the two-dimensional power spectrum. If the initial power spectrum of perturbations is the result of quantum mechanical fluctuations produced and amplified during inflation, then the shape of the anisotropy spectrum is coupled to the ratio of contributions from density (scalar) and gravitational wave (tensor) perturbations [21]. If the energy scale of inflation at the appropriate epoch is at the level of $\simeq 10^{16}$GeV, then detection of the effect of gravitons is possible, as well as partial reconstruction of the

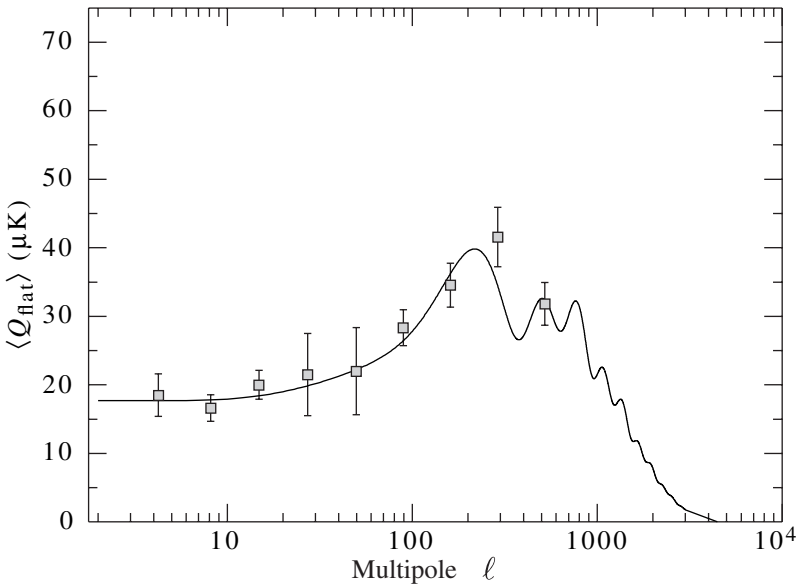

Figure 19.6: This is a binned version of the previous figure. To obtain this figure we took all reported detections, split the multipole range into equal logarithmic 'bins,' and calculated the weighted average in each bin. Although this is not a statistically rigorous procedure, the resulting figure gives a visual indication of the current consensus. It is also worth mentioning that there is no strong indication for excess scatter (above Gaussian) within each bin.

inflaton potential. If the energy scale is $\lesssim 10^{14}$GeV, then density fluctuations dominate and less constraint is possible.

Fits to data over smaller angular scales are often quoted as the expected value of the quadrupole $\langle Q\rangle$ for some specific theory, *e.g.* a model with power-law initial conditions (primordial density perturbation power spectrum $P(k) \propto k^n$). The full 4-year COBE DMR data give $\langle Q\rangle = 15.3^{+3.7}_{-2.8}$ μK, after projecting out the slope dependence, while the best-fit slope is $n = 1.2 \pm 0.3$, and for a pure $n = 1$ (scale-invariant potential perturbation) spectrum $\langle Q\rangle\,(n=1) = 18 \pm 1.6\,\mu$K [15,24]. The conventional notation is such that $\langle Q\rangle^2 / T_\gamma^2 = 5C_2/4\pi$, and an alternative convention is to plot the "band-power" $\sqrt{\ell(2\ell+1)C_\ell/4\pi}$). The fluctuations measured by other experiments can also be quoted in terms of $Q_{\rm flat}$, the equivalent value of the quadrupole for a flat ($n = 1$) spectrum, as presented in Fig. 19.5.

It now seems clear that there is more power at sub-degree scales than at COBE scales, which provides some model-dependent information on cosmological parameters [18,25], for example Ω_B. In terms of such parameters, fits to the COBE data alone yield $\Omega_0 > 0.34$ at 95% CL [26] and $\Omega_{\rm tot} < 1.5$ also at 95% CL [27], for inflationary models. Only somewhat weak conclusions can be drawn based on the current smaller angular scale data (see Fig. 19.5). A sample preliminary fit [28] finds $\Omega_0\, h^{1/2} \simeq 0.55 \pm 0.10$ ($\equiv 68\%$ CL).

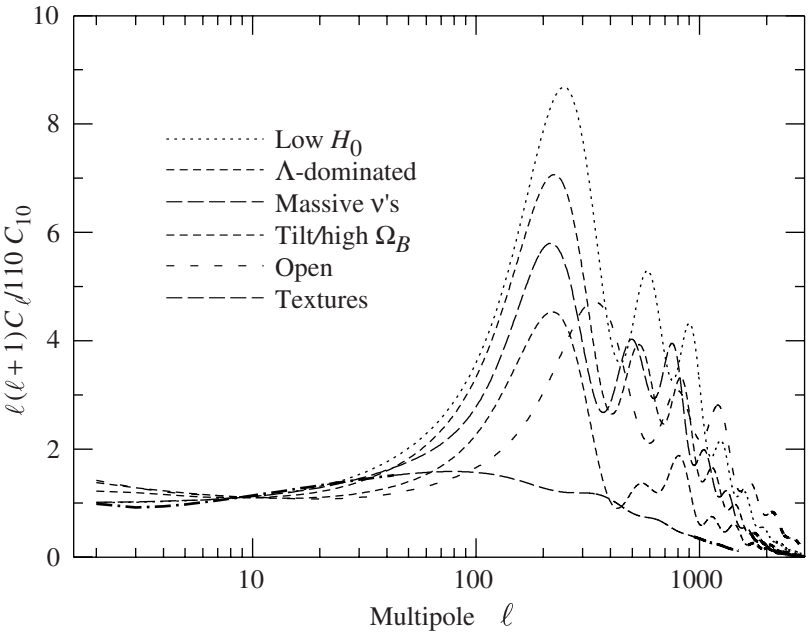

Figure 19.7: Examples of theoretically predicted $\ell(\ell+1)C_\ell$ or CMB anisotropy power spectra [22]. The plot indicates that precise measurements of the CMB anisotropy power spectrum could distinguish between models which are currently favored from galaxy clustering and other considerations. The textures model is from Ref. 23.

However, new data are being acquired at an increasing rate, with a large number of improved ground- and balloon-based experiments being developed. It appears that we are not far from being able to distinguish crudely between currently favored models, and to begin a more precise determination of cosmological parameters. A vigorous suborbital and interferometric program could map out the CMB anisotropy power spectrum to about 10% accuracy and determine several parameters at the 10 to 20% level in the next few years.

There are also now two approved satellite missions: the NASA Millimetre Anisotropy Probe (MAP), scheduled for launch in 2000; and the ESA Planck Surveyor, expected to launch around 2004. The improved sensitivity, freedom from earth-based systematics, and all-sky coverage allow a simultaneous determination of many of the cosmological parameters to unprecedented precision: for example, Ω_0 and n to about 1%, Ω_B and H_0 at the level of a few percent [29].

Furthermore, detailed measurement of the polarization signal provides more precise information on the physical parameters. In particular it allows a clear distinction of any gravity wave contribution, which is crucial to probing the $\sim 10^{16}$ GeV energy range. The fulfillment of this promise may await an even more sensitive generation of satellites.

References:

1. R.A. Alpher and R.C. Herman, Physics Today **41**, No. 8, p. 24 (1988).
2. A.A. Penzias and R. Wilson, Astrophys. J. **142**, 419 (1965);
   R.H. Dicke, P.J.E. Peebles, P.G. Roll, and D.T. Wilkinson, Astrophys. J. **142**, 414 (1965).
3. P.J.E. Peebles, "Principles of Physical Cosmology," Princeton U. Press, p. 168 (1993).
4. R.A. Sunyaev and Ya.B. Zel'dovich, Ann. Rev. Astron. Astrophys. **18**, 537 (1980).
5. M.T. Ceballos and X. Barcons, MNRAS **271**, 817 (1994).
6. C. Burigana, L. Danese, and G.F. De Zotti, Astron. & Astrophys. **246**, 49 (1991).
7. L. Danese and G.F. De Zotti, Astron. & Astrophys. **107**, 39 (1982);
   G. De Zotti, Prog. in Part. Nucl. Phys. **17**, 117 (1987).
8. J.G. Bartlett and A. Stebbins, Astrophys. J. **371**, 8 (1991).
9. E.L. Wright *et al.*, Astrophys. J. **420**, 450 (1994).
10. W. Hu and J. Silk, Phys. Rev. Lett. **70**, 2661 (1993).
11. D.J. Fixsen *et al.*, Astrophys. J. **473**, 576 (1996).
12. J.C. Mather *et al.*, Astrophys. J. **420**, 439 (1994).
13. M. Bersanelli *et al.*, Astrophys. J. **424**, 517 (1994).
14. A. Kogut *et al.*, Astrophys. J. **419**, 1 (1993);
    C. Lineweaver *et al.*, Astrophys. J. **470**, L28 (1996).
15. C.L. Bennett *et al.*, Astrophys. J. **464**, L1 (1996).
16. A. Kogut, G. Hinshaw, and A.J. Banday, Phys. Rev. **D55**, 1901 (1997);
    E.F. Bunn, P. Ferreira, and J. Silk, Phys. Rev. Lett. **77**, 2883 (1996).
17. G.F. Smoot *et al.*, Astrophys. J. **396**, L1 (1992).
18. D. Scott, J. Silk, and M. White, Science **268**, 829 (1995);
    W. Hu, J. Silk, and N. Sugiyama, Nature **386**, 37 (1996).
19. M. White, D. Scott, and J. Silk, Ann. Rev. Astron. & Astrophys. **32**, 329 (1994).
20. W. Hu, M. White, New Astron. **2**, 323 (1997).
21. J.E. Lidsey *et al.*, Rev. Mod. Phys. **69**, 373 (1997);
    D.H. Lyth, Phys. Rep., in press, hep-ph/9609431.
22. U. Seljak and M. Zaldarriaga, Astrophys. J. **469**, 437 (1996).
23. U.-L. Pen, U. Seljak, and N. Turok, Phys. Rev. Lett. **79**, 1611 (1997).
24. K.M. Górski *et al.*, Astrophys. J. **464**, L11 (1996).
25. A. Kogut and G. Hinshaw, Astrophys. J. **464**, L39 (1996).
26. K. Yamamoto and E.F. Bunn, Astrophys. J. **464**, 8 (1996).
27. M. White and D. Scott, Astrophys. J. **459**, 415 (1996).

28. C.H. Lineweaver and D. Barbosa, Astrophys. J., submitted, (1997) (astro-ph/9706077).

29. G. Jungman, M. Kamionkowski, A. Kosowsky, and D.N. Spergel, Phys. Rev. **D54**, 1332 (1996);

W. Hu and M. White, Phys. Rev. Lett. **77**, 1687 (1996);

J.R. Bond, G. Efstathiou, and M. Tegmark, MNRAS, in press (1997) (astro-ph/9702100);

M. Zaldarriaga, D. Spergel, and U. Seljak, Astrophys. J., in press (1997) (astro-ph/9702157).

CMB Spectrum References:

1. **FIRAS:** J.C. Mather *et al.*, Astrophys. J. **420**, 439 (1994);

D. Fixsen *et al.*, Astrophys. J. **420**, 445 (1994);

D. Fixsen *et al.*, Astrophys. J. **473**, 576 (1996).

2. **DMR:** A. Kogut *et al.*, Astrophys. J. **419**, 1 (1993);

A. Kogut *et al.*, Astrophys. J., Astrophys. J. **460**, 1 (1996).

3. **UBC:** H.P. Gush, M. Halpern, and E.H. Wishnow, Phys. Rev. Lett. **65**, 537 (1990).

4. **LBL-Italy:** G.F. Smoot *et al.*, Phys. Rev. Lett. **51**, 1099 (1983);

M. Bensadoun *et al.*, Astrophys. J. **409**, 1 (1993);

M. Bersanelli *et al.*, Astrophys. J. **424**, 517 (1994);

M. Bersanelli *et al.*, Astrophys. Lett. and Comm. **32**, 7 (1995);

G. De Amici *et al.*, Astrophys. J. **381**, 341 (1991);

A. Kogut *et al.*, Astrophys. J. **335**, 102 (1990);

N. Mandolesi *et al.*, Astrophys. J. **310**, 561 (1986);

G. Sironi, G. Bonelli, & M. Limon, Astrophys. J. **378**, 550 (1991).

5. **Princeton:** S. Staggs *et al.*, Astrophys. J. **458**, 407 (1995);

S. Staggs *et al.*, Astrophys. J. **473**, L1 (1996);

D.G. Johnson and D.T. Wilkinson, Astrophys. J. **313**, L1 (1987).

6. **Cyanogen:** K.C. Roth, D.M. Meyer, and I. Hawkins, Astrophys. J. **413**, L67 (1993);

K.C. Roth and D.M. Meyer, Astrophys. J. **441**, 129 (1995);

E. Palazzi *et al.*, Astrophys. J. **357**, 14 (1990).

CMB Anisotropy References:

1. **COBE:** G. Hinshaw *et al.*, Astrophys. J. **464**, L17 (1996).
2. **FIRS:** K. Ganga, L. Page, E. Cheng, and S. Meyers, Astrophys. J. **432**, L15 (1993).
3. **Ten.:** C.M.Gutiérrez *et al.*,Astrophys. J. **480**, L83 (1997).
4. **BAM:** G.S. Tucker *et al.*, Astrophys. J. **475**, L73 (1997).
5. **SP91:** J. Schuster *et al.*, Astrophys. J. **412**, L47 (1993). (Revised, see **SP94** reference.).
6. **SP94:** J.O. Gundersen *et al.*, Astrophys. J. **443**, L57 (1994).
7. **Sask.:** C.B. Netterfield *et al.*, Astrophys. J. **474**, 47 (1997).
8. **Pyth.:** S.R. Platt *et al.*, Astrophys. J. **475**, L1 (1997).
9. **ARGO:** P. de Bernardis *et al.*, Astrophys. J. **422**, L33 (1994);
   S. Masi *et al.*,Astrophys. J. **463**, L47 (1996).
10. **IAB:** L. Piccirillo and P. Calisse, Astrophys. J. **413**, 529 (1993).
11. **MAX:** S.T. Tanaka *et al.*, Astrophys. J. **468**, L81 (1996);
    M. Lim *et al.*, Astrophys. J. **469**, L69 (1996).
12. **MSAM:** E.S. Cheng *et al.*, Astrophys. J. **456**, L71 (1996);
    E.S. Cheng *et al.*, Astrophys. J., in press (1997) (astro-ph/9705041).
13. **CAT:** P.F.S. Scott *et al.*, Astrophys. J. **461**, L1 (1996).
14. **WD:** G.S. Tucker, G.S. Griffin, H.T. Nguyen, and J.B. Peterson, Astrophys. J. **419**, L45 (1993).
15. **OVRO:** A.C.S. Readhead *et al.*, Astrophys. J. **346**, 566 (1989).
16. **SuZIE:** S. E. Church *et al.*, Astrophys. J. **484**, 523 (1997).
17. **ATCA:** R. Subrahmayan, R.D. Ekers, M. Sinclair, and J. Silk, Monthly Not. Royal Astron. Soc. **263**, 416 (1993).
18. **VLA:** B. Partridge *et al.*, Astrophys. J. **483**, 38 (1997).